A New Air Velocity Standard by Using LDV and a Wind Tunnel at CMS

Cheng-Tsair Yang, Jeng-Yuan Chen, and, Jiunn-Haur Shaw
(Center for Measurement Standards/ITRI, Hsinchu 300, Taiwan, China)

Abstract Though air speed measurements are daily routine in many industries, calibration is still a problem due to the lack of standard. Though the Center for Measurement Standards (CMS) has established a calibration facility since 1997, the block effects resulted from small wind tunnel section constrained the devices to be calibrated. In this paper, a facility comprises a redesigned wind tunnel and a LDV with expanded lens was tested of its performance to estimate its uncertainty of measurement. Firstly, the expanded LDV probe was readjusted of its beam crossings and calibrated of its fringe spacing. This improved the uniformity of fringe pattern in the measuring volume to obtain accurate fringe spacing that serves as velocity coefficient and to reduce the uncertainty of LDV measurement to be less than 0.1%. The tunnel was tested under air speed from 0.5 m/s to 25 m/s. Turbulence intensity, long-term flow stability, and uniformity of velocity profiles are all considered as significant sources of measurement uncertainty. The uncertainty analysis indicated that the relative expanded uncertainty for regular calibration could be less than 0.5%.

Keyword: Air speed, LDV, Wind tunnel, Anemometry

1. Introduction

Air-speed measurements are widely applied, including meteorology research, industrial ventilation and environmental concerns. The calibration of anemometry has been widely practiced in wind tunnel in which the air speed is mostly measured by means of pressure-difference transformation; the traceability, however, is not clearly confirmed yet.

In Taiwan, China, the present requirement for calibration of anemometry follows the code CNS 8456[1], in which the calibration of anemometry is performed in wind tunnel and the air speed of larger than 5 m/s is measured by pitot tube, but standard for lower air speed is limited due to the non-linear nature of Bernoulli's law. LDV is advantaged by its non-invasion and potential traceability. NIST also adopted LDV as velocity standards to calibrate anemometry in wind tunnel [2-3]. This approach established acceptable traceability and suited for wide-range air speed. Though this approach gradually adopted in many NMIs, the intercomparisons [4-5] indicated that improvement in test facilities, measurement standard and test tunnel, is an essential issue.

This paper firstly described the newly implemented wind tunnel for air-speed calibration and the employed LDV that was expanded of its lens for incident beams. The LDV was then steered of its incidence beams to reach optimal fringe pattern according to the previous procedure [6]. Then, the wind tunnel was measured of its long-tem stability, turbulence and velocity profile at velocity ranging from 0.5 m/s to 25 m/s. The flow characteristics near the contraction nozzle was specially analyzed to evaluate proper region for probe locating and to estimate the uncertainty of measurement. The results shows relative expanded uncertainty of measurement for air-speed calibration could be reached less than 0.5%.

2. Measurement Facilities

A wind tunnel accompanying with a turn-key LDV has been established for anemometry calibration at CMS since 1997. The LDV probe has been re-adjusted of its beam alignment and calibrated of its fringe spacing before and after the beam re-adjustment, thus that the variation of fringe spacing was improved from 3% down to 0.28% in the measuring volume[6]. However, the tunnel section of 162 mm ×162 mm was not sufficient to avoid significant error from blockage

effect when calibrating vane-type anemometry. In addition, the operational air-speed in the wind tunnel was maximized at 15 m/s that was not sufficient for some requirement. Therefore, new wind tunnel was demanded and implemented to meet the requirement.

2.1 Wind tunnel

Considering the available room for wind tunnel, the extension of air-speed, and the requirement to reduce blockage effects, an open-loop wind tunnel with a semi-opened test section was designed and implemented referring to that in PTB [5]. Shown in figure 1 is the sketch of the wind tunnel, which comprises a flow conditioning section, a test section and a fan diffusion section. The air is sucked into the test section through the conditioning section in which the flow is uniformed and the turbulence is suppressed by use of three fine mesh screens and a contraction nozzle. The diameter of outlet of the contraction nozzle is 200 mm, and the test section is 800 mm ×800 mm in cross section and 1000 mm in length. Both the sidewalls of the test section can be opened to properly install the anemometry under calibration. Air is then sucked out through the diffusion section with inlet diameter of 300 mm.

The blower is powered by a 1.5 Kw AC motor and is controlled by a frequency converter to generate steady rotation rate and hence steady air speed. For slow air speed, a perforated circular plate can be inserted at the inlet of the fan diffusion section to increase pressure drop. In this paper, range of steady air speed was to be determined firstly; and the flow profiles near the nozzle outlet were to be measured so that proper region for locating the probe of anemometry could be determined. The designed air speed of this wind tunnel is 0.5 m to 25 m/s for the present test and is expected to be lowered down by the use of pressure-drop plate.

2.2 LDV system

Because the test section of the new wind tunnel is much larger that that of our old one, the focal length of the LDV probe was not long enough so that new lens or beam expander was required. Beam expander was adopted to keep good feature of the measuring volume and hence good scattering signals. Of specifications, the nominal focal length is 450 mm, and the fringe spacing was calculated as 1.921 μm based on given beam angle and optical wavelength of 514.5 nm. Shown in figure 2 is the photo of arrangement of implemented wind tunnel and expanded LDV

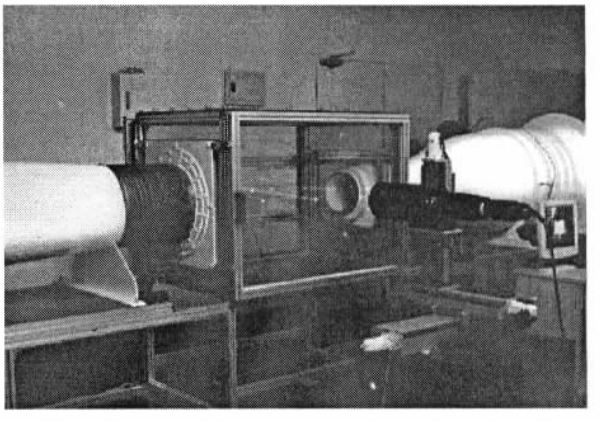

Fig. 2 Photo of the new wind tunnel and LDV

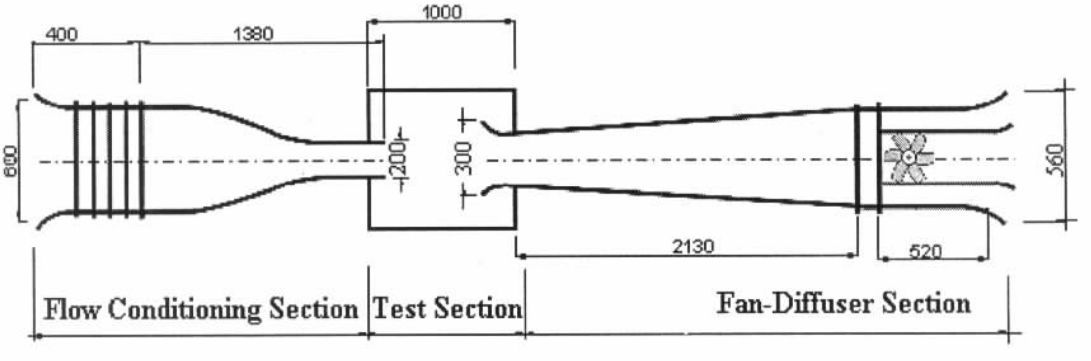

Fig. 1 Sketch of the new wind tunnel (unit: mm)

Following the calibration and analysis procedure [6] for our LDV probe before beam expanding, the expanded LDV fiber probe were firstly adjusted of its distribution of fringe spacing in the measuring volume by realigning the crossing beams. Theoretically, due to misalignment of incident Gaussian beams, the fringes are not uniformly distributed in the measuring volume as expressed in Eq.(1) and as instanced in figure 3 [6], where d is the local fringe spacing, Z and X is the longitudinal and traversal coordinates respectively.

$$d=\frac{\lambda}{2\sin\alpha}\left[1+\frac{((x_1z_1/z_1^2+z_{R1}^2)-(x_2z_2/z_2^2+z_{R2}^2))}{2\tan\alpha(x_1z_1/z_1^2+z_{R1}^2)-(x_2z_2/z_2^2+z_{R2}^2))}\right] \quad \text{.....(1)}$$

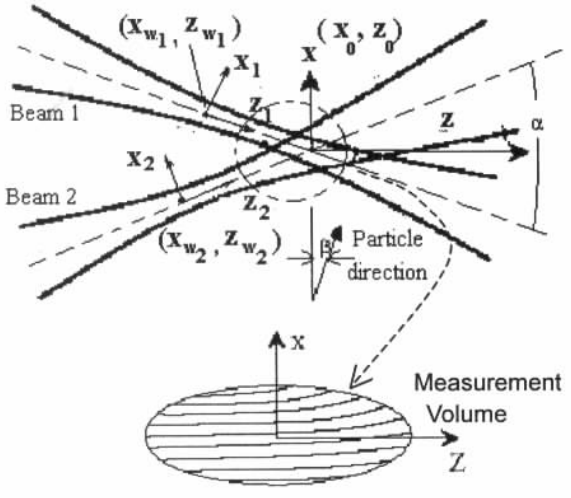

Fig. 3 Instance of the result of misaligned incident Gaussian beams.

A validated spinning glass disk of 200 mm in diameter was adopted as reference standard. Because the tangential velocity at the rim surface of the thick disk equals the product of Doppler frequency and local fringe spacing, i.e. $V = f_D \cdot d_f$, measuring that the Doppler frequency at different alignment conditions and specified spinning speed can obtain the estimation of fringe variance. As shown in figure 4, the curve of legend 0 is the fringe variation along long axial in the measuring volume. When re-crossed the incident beams at about 1.85 mm away from the original crossing point, the uniformity was much improved to a minimal fringe variation about 0.6% as shown in figure 5. In the case without beam expander, the variance had been improved from 3% to 0.3%.

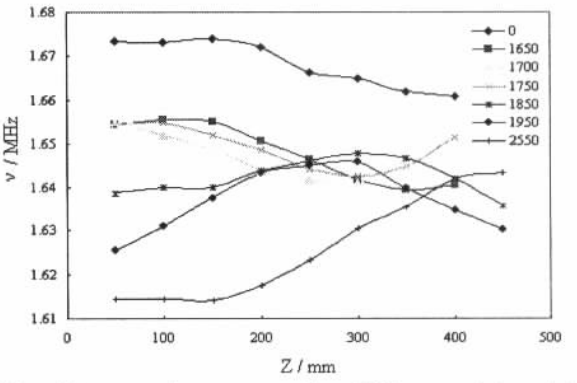

Fig. 4 Frequencies measured at different axial positions (Z). These curves also represent the variance of fringe patterns. The legends denote the displacements of re-crossed measuring volumes to the original position in μm.

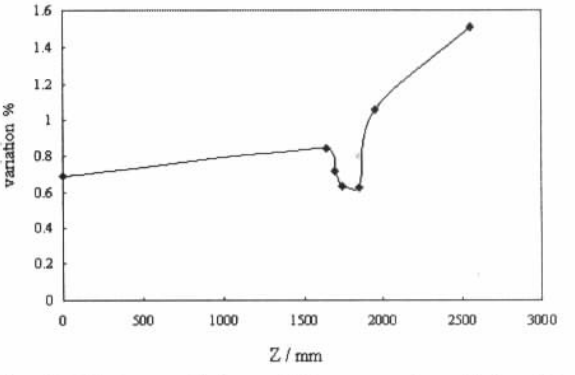

Fig. 5 Relative variation of fringe spacing, derived from figure 4.

Based on the reset probe condition, the measuring volume was determined of its mean fringe spacing from measurements at different spinning speed. The results of green component (514.5 nm) is shown in figure 6, deriving a mean fringe spacing D to be 1.9225 μm, which is 0.08% deviated from the nominal value, with uncertainty of less than 0.1%.

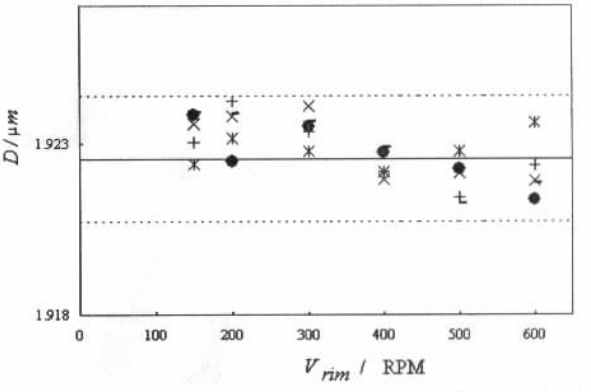

Fig. 6 Estimated fringe spacing under different spinning speed (five runs).

3. Results, Analysis and Discussions

To determine proper region to locate the probe of anemometry under test, the velocity profile near the outlet of contraction nozzle was measured by using the calibrated LDV. Meanwhile, the measurement uncertainty in calibrating anemometry can hence be derived from the adopted LDV and the characteristics of measured velocity profiles.

3.1 Wind tunnel flow profiles

Measurements were made at various velocities. The profile for mean velocity of 13.34 m/s at the outlet of the nozzle is shown in figure 7 which illustrates the top-hat profile as expected. The profiles along vertical diameter shown in figure 8 exhibit the extension of nozzle flow, where X is the distance from the outlet. After obtaining flow profiles at different velocities and different locations, the positions for performing calibration can be determined by the analysis in the following paragraph.

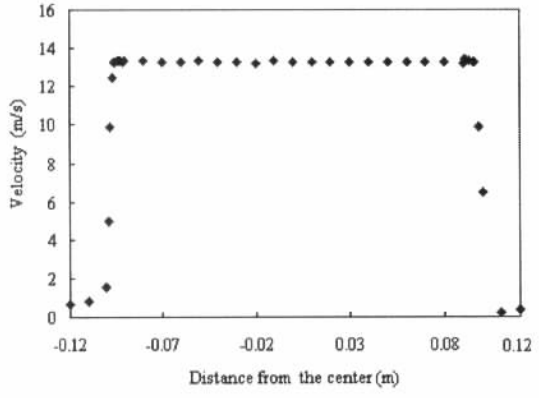

Fig.7 Top-hat velocity profile (mean = 13.34 m/s) at the outlet of contraction nozzle(X = 0).

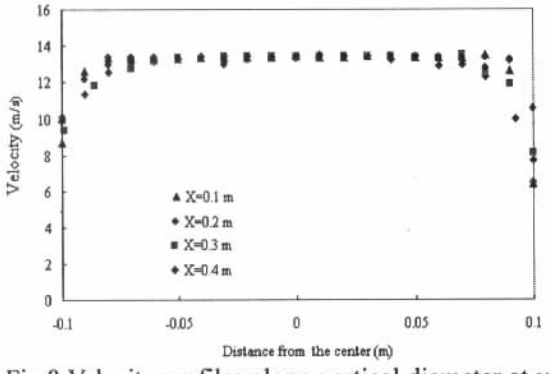

Fig.8 Velocity profiles along vertical diameter at various distance to the outlet plane X = 0.1 m, 0.2 m, 0.3 m, and 0.4 m, respectively.

Numerical code CFD-ACE$^+$ was also employed in the flow research for comparison. Finite difference approach was used to resolve k-ε RNG turbulence model; while the measured velocities at the outlet surface of contraction nozzle served as the boundary condition. SIMPLE algorithm with second order upwind-differencing scheme was used to solve the spatial discretized problem in computational domain. The result shown in figure 9 is the central-plan velocity distribution in the test section at mean velocity = 13.34 m/s. Comparison of CFD simulation with LDV measurement is shown in figure 10 that show good agreement to each other.

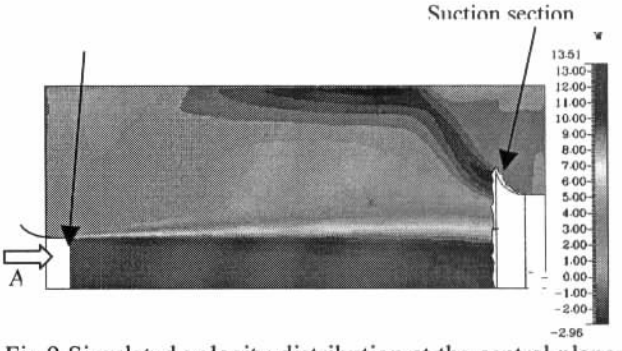

Fig.9 Simulated velocity distribution at the central plane in the test section between contraction nozzle and suction section.

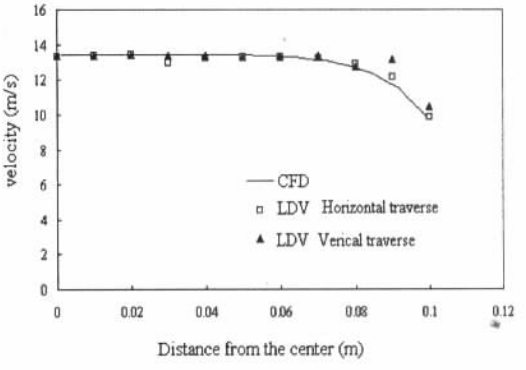

Fig.10 Comparison between CFD simulation and LDV measurement.

3.2 Uncertainty analysis

The uncertainty of the calibration for air-speed measurement considered both the influences of LDV measurement capability, flow profiles and the performance of wind tunnel. Therefore, the measured velocity in wind tunnel is modified as follows,

$$V_{tunnel} = V_{ldv} \times \delta \times \varepsilon \quad (2)$$

where V_{ldv} denotes the measured velocity, V_{tunnel} is the modified velocity, δ and ε are factors due to flow fields distribution and the characteristics of wind tunnel, respectively. The uncertainty of V_{tunnel}, denoted as $u_c(V_{tunnel})$ can thus be expressed as

$$u_c^2(V_{tunnel}) = [c_1 u(V_{ldv})]^2 + [c_2 u(\delta)]^2 + [c_3 u(\varepsilon)]^2 \quad (3)$$

where $u(V_{tunnel})$, $u(\delta)$, $u(\varepsilon)$ are the respective standard uncertainties; while c_i are the sensitivity coefficients. Then, Eq.(3) can be rewritten into a relative form as

$$\frac{u(V_{tunnel})}{V_{tunnel}} = \left(\left(\frac{u(V_{ldv})}{V_{ldv}}\right)^2 + \left(\frac{u(\delta)}{\delta}\right)^2 + \left(\frac{u(\varepsilon)}{\varepsilon}\right)^2\right)^{1/2} \quad (4)$$

As mentioned, the relative standard uncertainty of LDV system $u(V_{ldv})/V_{ldv}$ is 0.1% with coverage factor k of 2.26 [7]. The effects from flow field and wind tunnel were investigated from experiments.

3.2.1 Effects due to flow-field property

The relative standard uncertainty of flow-field property includes particle lag, velocity sampling bias, and turbulence intensity. The estimation of particle lag and sampling bias referred to Fry [8] and Yang [9]. Shown in figure 11 is the turbulence intensity at 10 mm downstream of the nozzle exit for various air speeds, indicates that the turbulence intensity ranges from 1.73% to 0.81%. For the critical condition at V = 1.062 m/s, the relative standard uncertainty due to turbulence is 0.055%.

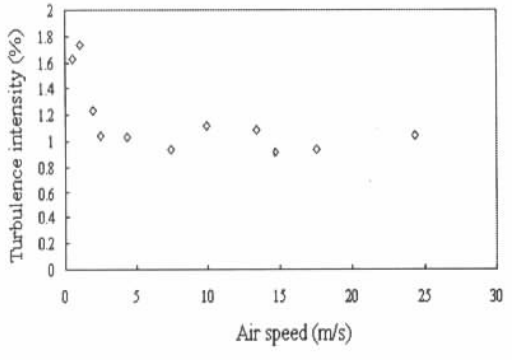

Fig. 11 Turbulence intensity for various air speeds at 100 mm downstream of the contraction nozzle.

3.2.2 Long-term stability of flow in wind tunnel

The stability of flow in the test section is also critical in case data of the anemometry and LDV are not acquired at the same time. Shown in figure 12 is the long-term stability test of air speed in wind tunnel. For average velocity of 24.36 m/s, the standard variation in one hour is less than 0.15%; meantime, for average velocity of 0.52 m/s the flow stability is less than 0.9%. This implies that the calibration uncertainty for lower air speed should be larger than that for higher air speed.

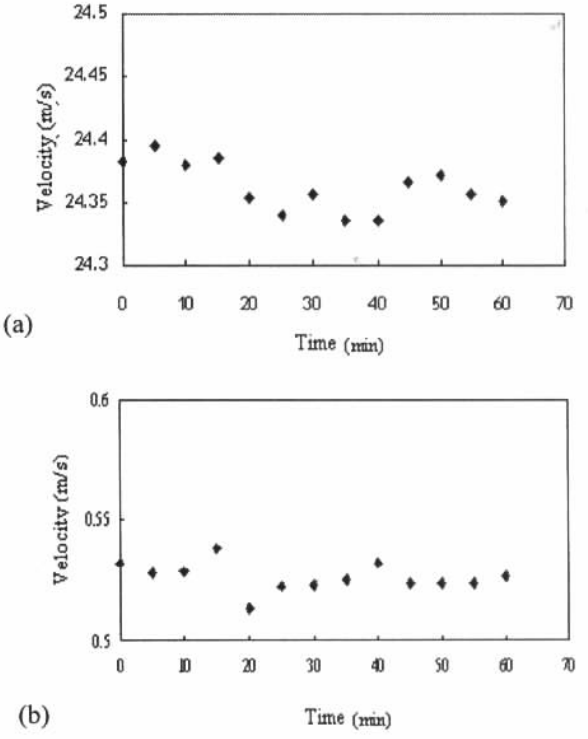

Fig. 12 Long-term velocity stability test at mean velocity (a) 24.36 m/s and (b)0.52 m/s, respectively.

3.2.3 Short-term characteristics of flow in the wind tunnel

The characteristics of the wind tunnel here are defined as the uniformity and short-term stability of velocity distributions in a destined region near the exit of the contraction nozzle for the insertion of anemometry under calibration. Some velocity distributions at 100 mm downstream for various air speeds are shown in figure 13; while some distributions along center lines of test section are shown in figure 14. Based on all measured profiles

from 0.5 m/s to 25 m/s, vertically and horizontally (not shown), the standard deviation of velocities in the region of X = 0 to 100 mm and R = 0 to 40 mm was < 0.14% that results in a relative standard uncertainty $u(\varepsilon)/\varepsilon$ to be 0.23% for anemometry calibration. We also considered the situations that the probe could be only located outside the core region or the probe is vane-type, the destined region should be extended to R = 0 to 70 mm with standard deviation of velocity <0.23% that results in a relative standard uncertainty $u(\varepsilon)/\varepsilon$ to be 0.35%.

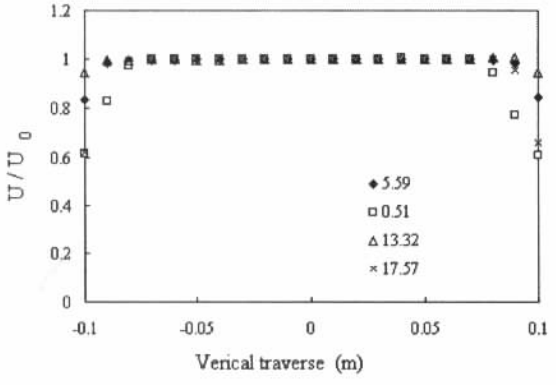

Fig. 13 Velocity distributions in the central plane at distance of 100mm downstream the exit of nozzle

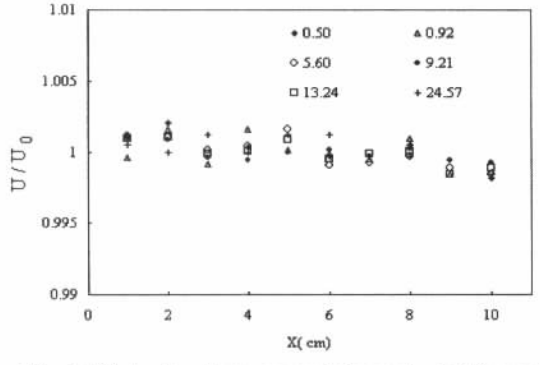

Fig. 14 Velocity along central line of wind tunnel

As mentioned that the destined region for anemometry calibration depends on the probe under test. Therefore, we defined a regular region, X = 0 to 100 mm and R = 0 to 40 mm, and a extended region, X = 0 to 100 mm and R = 0 to 70 mm, as sketched in figure 15. Substituting the uncertainty components listed in Table 1 into Eq.(4), the general estimated relative expanded uncertainty of air-speed measurement in regular region was 0.5% at 95% confidence level. Similar estimation for extended region resulted in relative expanded uncertainty of air-speed measurement in the region to be 0.73% at 95% confidence level.

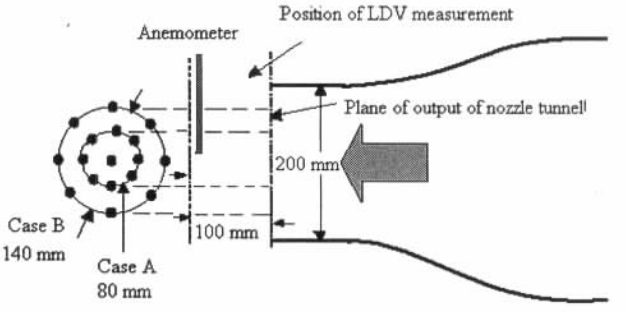

Fig. 15 Designated regions for positioning probe of anemometry: regular region (case A) and extended region (case B).

Table 1. Components in uncertainty analysis

component	sources	$u(x_i)/x_i$ %	ν_x
$[\frac{u(V_{ldv})}{V_{ldv}}]$	**LDV facility**	0.050	9.5
$[\frac{u(\delta)}{\delta}]$	**Flow field**	0.055	1066
	Particle lag	0	∞
	Sampling bias	0.01	∞
	Turbulence	0.0548	999
$[\frac{u(\varepsilon)}{\varepsilon}]$	**Wind tunnel effects**	0.230	23
	Vertical flow profile	0.141	8
	Horizontal flow profile	0.129	4
	Axial velocity change	0.128	9

4. Conclusion

In this paper, a facility for anemometry calibration that comprises a wind tunnel and a LDV with expanded lens was implemented and tested of its performance. Both the LDV and wind tunnel capability were considered the sources of uncertainty measurement. Therefore, the LDV was firstly calibrated of its fringe spacing that serves as velocity coefficient by realigning the crossing beams and comparing with a standard horizontally rotating disc. Then the velocity profiles, turbulence intensity, and long-term stability of the air flow were measured to estimate the influences. Based on the flow-field characteristics, the space for installing probe of anemometry was confined to reach desirable uncertainty in calibration. For general small probe that was calibrated at air speed of 0.5 m/s to 25 m/s,

the relative expanded uncertainty was 0.5% at 95% of confidence level ; for larger probe, it was 0.73% at 95% of confidence level.

Acknowledgement

The authors are grateful to the Bureau of Standards, Metrology and Inspection (BSMI), Taiwan, China , for support of this work under grant No. NBS-NML-001-P501.

Reference

[1] Calibration Method for Portable Thermal Anemometry, *BSMI Taiwan, China*, CNS 8456.

[2] Bear, V.E., New Primary Standards for Air Speed Measurement at NIST, *NCSL Workship and Symposium*, 1999: 413-421

[3] Mease N.E., Cleveland W. G. Mattingly G.E., Air speed calibration at the national institute of standard and technology, *NIST*, MD 20899.

[4] Intercomparison of Anemometers, *EUROMET Project No. 388*, 1999

[5] Sánchez, J.R., Müller, H., Care, I., Seynhaeve, J.M., Cordier, Y., LDA Calibration Sensor Intercomparison, *12th Int'l sym. on Application of laser techniques to fluid mechanics*, 2004: 22.5

[6] Yang, C.T., Wu, M.C., and Chuang, H.S., Adjustment and evaluation of an LDV probe for accurate flow measurement, *Optics and Lasers in Engineering*, 2002, 38: 291-304.

[7] Yang, C.T, Wu, M.C., Chuang, H.S., Measurement system validation procedure of a standard spinning disc for LDV calibration, *Center for Meas. Standards*, 2000, 07-3-89-0100.

[8] Fry, D.J., Three-Component Laser Doppler Velocimetry Towing Tank System Measurement Error, *DTNSRDC*, 1985, SPD-1163-03.

[9] Yang, C.T., Tip-vortex flow field and its induced cavitation, *Ph.D thesis (in Chinese), National Taiwan University*, 1994